Hernández Teruel, A.; Pérez-Esteve, É.; González-Álvarez, I.; González-Álvarez, M.; Costero Nieto, AM.; Ferri, D.; Gaviña, P.... (2019). Double Drug Delivery Using Capped Mesoporous Silica Microparticles for the Effective Treatment of Inflammatory Bowel Disease. Molecular Pharmaceutics. 16(6):2418-2429. https://doi.org/10.1021/acs.molpharmaceut.9b00041

Double drug delivery using capped mesoporous silica microparticles for the effective treatment of Inflammatory Bowel Disease

Adrián H Teruel,[1,2] Édgar Pérez-Esteve,[1] Isabel González-Álvarez,[3] Marta González-Álvarez,[3] Ana M. Costero,[1,2,4] Daniel Ferri,[1,2,4] Pablo Gaviña,[1,2,4] Virginia Merino,[5] Ramón Martínez-Máñez,[1,2,6,7,] and Félix Sancenón[1,2,6,7]*

[1] Instituto Interuniversitario de Investigación de Reconocimiento Molecular y Desarrollo Tecnológico (IDM), Universitat Politècnica de València, Universitat de València, Camino de Vera s/n, 46022 Valencia, Spain.

[2] CIBER de Bioingeniería, Biomateriales y Nanomedicina (CIBER-BBN).

[3] Departamento de Ingeniería, Sección de Farmacia y Tecnología Farmacéutica, Universidad Miguel Hernandez, 03550, Alicante, Spain.

[4] Departamento de Química Orgánica, Universitat de València, Doctor Moliner 50, Burjassot, 46100, Valencia, Spain.

[5] Departamento de Farmacia y Tecnologia Farmacéutica, Universitat de València 46100, Valencia, Spain.

[6] Unidad Mixta de Investigación en Nanomedicina y Sensores. Universitat Politècnica de València, Instituto de Investigación Sanitaria La Fe, Valencia, Spain.

[7] Unidad Mixta UPV-CIPF de Investigación en Mecanismos de Enfermedades y Nanomedicina, València, Universitat Politècnica de València, Centro de Investigación Príncipe Felipe, Valencia, Spain.

KEYWORDS: Mesoporous silica microparticles, gated materials, smart drug delivery materials, colon targeted release, inflammatory bowel disease

ABSTRACT

Silica mesoporous microparticles loaded with both rhodamine B fluorophore (**S1**) or hydrocortisone (**S2**), and capped with an olsalazine derivative, are prepared and fully characterized. Suspensions of **S1** and **S2** in water at an acidic and a neutral pH show negligible dye/drug release, yet a notable delivery took place when the reducing agent sodium dithionite is added due to a hydrolysis of an azo bond in the capping ensemble. Besides, olsalazine fragmentation induced 5-aminosalicylic acid (5-ASA) release. *In vitro* digestion models show that **S1** and **S2** solids are suitable systems to specifically release a pharmaceutical agent in the colon. *In vivo* pharmacokinetic studies in rats show a preferential rhodamine B release from **S1** in the colon. Moreover, a model of ulcerative colitis is induced in rats by oral administration of 2,4,6-trinitrobenzenesulfonic acid (TNBS) solutions, was also used to prove the efficacy of **S2** for colitis treatment. The specific delivery of hydrocortisone and 5-ASA from **S2** material to the colon tissue in injured rats markedly lowers the colon/body weight ratio and the clinical activity score. Histological studies showed a remarkable reduction in inflammation, as well as an intensive regeneration of the affected tissues.

1. INTRODUCTION

Inflammatory bowel disease (IBD) is an idiopathic autoimmune, inflammatory and chronic disease. There are essentially two main IBD subtypes: ulcerative colitis (UC) and Crohn's disease (CD). However this classification is not always obvious because clinical and pathologic features substantially overlap.[1-11] The IBD etiology is still poorly understood, but all the facts indicate a multifactorial origin, where genetics, environmental, and intestinal microbiota are the main factors. Since IBD are chronic diseases with a low mortality, continuous incidence or newly diagnosed patients increase the number of prevalent cases. The whole costs of IBD are quite overwhelming. More than 1,000,000 of people are estimated to suffer from IBD (just in USA), and only the direct medical costs exceeded US$ 6 billion in 2004.[12,13] In Canada over 200,000 people suffer IBD, with more than CDN$ 1.2 billion spent on direct healthcare costs per year.[14] Moreover, over 3,000,000 of European patients suffer from IBD, and the direct healthcare spent is calculated to be over €5 billion per year.[15] The biggest contributors in these healthcare-related costs are pharmaceuticals, hospitalizations, surgery and outpatient care.[16] Moreover, non-direct IBD costs (e.g. lost work productivity), exceed even direct costs. Besides, in the last decades, developing countries (in Middle East, South America and Asia) have seen an important emergence on IBD incidence and prevalence.[17-21]

Considering together the above mentioned facts, plus the lack of a definitive solution available on the market, the development of new strategies to treat IBD are of interest. Conventional IBD therapy includes 5-aminosalicylic acid (5-ASA), corticosteroids and immunosuppressants.[22] Steroids were the cornerstone of ulcerative colitis therapy for several years due to their proved anti-inflammatory efficacy. However, the therapeutic efficacy of steroids in IBD is controversially affected by serious secondary effects. As an alternative, in the last decade, biological agents (especially anti-TNF (tumor necrosis factor) therapies) have been introduced to be used in UC/CD patients who failed conventional therapy.[23,24] As an alternative to these therapies, nano- and microparticle as drug carriers for oral administration have been tested in experimental colitis models to increase drug efficacy.[25-27] However, among different nano- and microparticles, mesoporous silica particles (MSPs) have still been barely studied as carries for IBD treatment.[28,29] As containers of selected cargo molecules, mesoporous silica nano- or microparticles have been broadly studied in recent decades for their promising

characteristics, such as their biocompatibility, large specific surface areas (up to 1200 m^2 g^{-1}), customizable pore size (within the 2-10 nm diameter range), large load capacity, homogeneous porosity, tunable particle, inertness and good thermal stability. Compared to organic nanocarriers, mesoporous silica materials are generally more resistant to pH, variations in temperature and mechanical stress, which renders them improved capability to protect molecules and biomolecules when they come into contact with body fluids. Besides, MSPs can be decorated with selected molecular or supramolecular entities to either enhance selectivity to cells and tissues or control the delivery of certain entrapped cargos at will using specific external stimuli.[30-38]

Considering the urge to find a better solution for the treatment of IBD, we report herein the synthesis and characterization of mesoporous silica microparticles loaded with rhodamine B or hydrocortisone and capped with an olsalazine derivative (see Scheme 1). As a consequence of the grafting of bulky olsalazine groups on the external surface of the loaded inorganic framework, the prepared microparticles are unable to release the entrapped cargo. However, when a reducing agent such as sodium dithionite (which mimic the azoreductase enzyme activity of the colon microbiota) is present the olsalazine derivative is hydrolyzed and yields 5-aminosalicylic acid (5-ASA). This hydrolysis process induces pore opening and delivery of the entrapped cargo (i.e. rhodamine B or hydrocortisone). As a novelty, one of the prepared mesoporous microparticles is able to deliver two drugs at the same time; i.e. hydrocortisone (located in the pores of the inorganic silica scaffold) and 5-ASA (product of the hydrolysis of the gating olsalazine). The effect of the co-delivery of both drugs is studied in an *in vivo* IBD rat model. The information obtained by parameters such as the clinical activity score, the colon/body weight ratio and the histological evaluation, confirms the usefulness of these microparticles system to treat IBD.

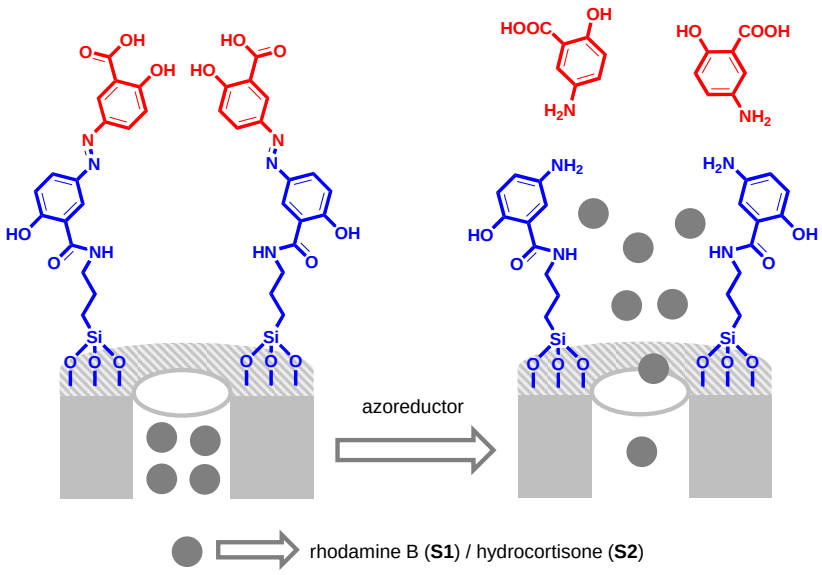

Scheme 1. Representation of rhodamine B (**S1**) or hydrocortisone (**S2**) loaded silica mesoporous particles capped with an olsalazine derivative. Delivery of both cargos (rhodamine B or hydrocortisone) is induced by an azoreductor.

2. EXPERIMENTAL SECTION

2.1. General Techniques. Transmission electron microscopy (TEM), scanning transmission electron microscopy (STEM), thermogravimetric analysis (TGA), N_2 adsorption-desorption isotherms, powder X-ray diffraction (PXRD), Fourier transform infrared spectroscopy (FTIR), nuclear magnetic resonance (NMR), fluorescence spectroscopy and HPLC techniques were used in order to characterize the prepared materials. The instruments used were: JEOL JEM-1010 microscope for TEM images acquisitions. Bruker D8 Advance diffractometer (CuK_α radiation) for PXRD measurements. TGA/SDTA 851e Mettler Toledo balance for TGA, using air (80 mL/ min) as an oxidant atmosphere with the following heating program: heating ramp of 10 °C/min from 393 to 1273 K, then an isothermal heating step at 1273 K for 30 minutes. Micromeritics ASAP 2010 automated analyzer for N_2 adsorption-desorption isotherms recording, samples were degassed at 120 °C in a vacuum overnight. The specific surface areas were calculated from the adsorption data within the low-pressure range using the BET (Brunauer–Emmett–Teller) model. Pore size was determined following the BJH (Barrett-Joyner-Halenda) method. Bruker AV400 spectrometer to measure ^{1}H NMR spectra. Bruker Tensor 27 equipment to record infrared spectra. PerkinElmer EnSpire Multimode Plate Reader for

fluorescence measurements. Hitachi LaChrom Elite HPLC with a UV detector (L-2400) and an auto-sampler (L-2200) for HPLC analysis, using Kromaphase 100 C18 column (150 mm × 4.6 mm i.d., 5 µm particle size) for separations.

2.2. Chemicals. The chemicals tetraethylorthosilicate (TEOS), 1-hexadecyltrimethylammonium bromide (CTABr), sodium hydroxide (NaOH), triethanolamine ($TEAH_3$), *N*-hydroxysuccinimide (NHS), *N*,*N*′-dicyclohexylcarbodiimide (DCC), (3-aminopropyl)triethoxysilane, rhodamine B, triethylamine, hydrocortisone, sodium dithionite and 2,4,6-trinitrobenzene sulfonic acid solution (TNBS) were purchased from Sigma-Aldrich. Sodium acetate anhydrous, potassium chloride, sodium dihydrogen phosphate, potassium dihydrogen phosphate, disodium hydrogen phosphate, hydrochloric acid and all the solvents were provided by Scharlab. Olsalazine sodium salt (Mordant yellow 5) was purchased from Molekula. The animal facilities supplied isoflurane pentobarbital (dolethal®). All the chemicals were used as received.

2.3. Synthetic protocols.

2.3.1. ***Synthesis of mesoporous silica microparticles (S0).*** We used the "atrane route" to synthesize the micro-sized mesoporous silica particles.[39] In a typical synthesis, $TEAH_3$ (25.8 g, 0.17 mol) and sodium hydroxide (2 mL, 6 M) were mixed and the obtained solution was heated to 120 ^{o}C and then cooled down to 70 ^{o}C. Afterward, TEOS (11 mL, 0.045 mol) was added to the initial solution that was then heated to 120 ^{o}C. Next, solution was left to cool down and the surfactant CTABr (4.7 g, 0.013 mol) was added at 118 °C. At this time, distilled water (80 mL) was slowly added under vigorous stirring at 70 °C. The resultant mixture was aged at 100 ^{o}C in an autoclave for 24 h. The obtained powder was filtrated and washed with abundant water. In the last step of the protocol, the solid is dried at 70 °C. To obtain the solid (**S0**), a calcination process at 550 ºC is performed in an oxidant atmosphere during 5 h in order to remove the surfactant template from the as-synthesized microparticles.

2.3.2. ***Synthesis of 1a.*** Olsalazine sodium salt (0.5 g, 1.65 mmol) was dissolved in an acidic solution of pH≈0 (28.5 mL of distilled water and 1.5 mL 37% HCl solution). The resultant solution was stirred for 5 min at room temperature and then centrifuged. The supernatant was discarded and the resulting protonated product (**1a**, 0.45 g, 1.49 mmol, 90% yield) was recovered and dried at 70 ^{o}C for 24 h. This protocol was repeated 4 times.

2.3.3. *Synthesis of 1.* DCC (1.04 g, 5 mmol) and NHS (0.59 g, 5 mmol) were dissolved in anhydrous THF (25 mL). Afterward, this mixture was then poured over a solution of compound **1a** (1.53 g, 5 mmol) in anhydrous THF (25 mL). The crude reaction was stirred during 5 h at room temperature in an argon atmosphere. A white-yellowish precipitate of dicyclohexylurea (DCU) was discarded by centrifugation. The supernatant was left stirring for 15 h in an argon atmosphere at room temperature. After 15 h the crude reaction was recentrifuged to remove the newly formed DCU. Then, (3-aminopropyl)triethoxysilane (**1b**, 1.2 mL, 5 mmol) was slowly added to the crude reaction and was stirred for a further 24 h period (room temperature, argon atmosphere). The solvent was removed using a rotary evaporator to isolate the final product **1** (yellow-orange oil, 2.05 gr, 4.05 mmol, 80% yield). ^{1}H NMR (400 MHz, DMSO-D_6): δ = 8.31 (d, 2H), 7.98 (dd, 2H), 7.05 (d, 2H), 3.65 (m, 6H), 3.36 (t, 2H), 1.67 (m, 2H), 1.17 (m, 9H), 0.68 (t, 2H) ppm. HRMS-EI *m/z*: calcd for $C_{23}H_{31}N_3O_8Si$: 505.1880; found: 436.3410 (M-2(CH_3CH_2OH)+Na) and 391.2828 (M-3(CH_3CH_2OH)+Na).

2.3.4. *Synthesis of S1.* Solid **S0** (1 g) was suspended in a THF (40 mL) solution containing rhodamine B (400 mg, 0.8 mmol/g of solid) under argon. Suspension was stirred at room temperature overnight. Afterward, compound **1** (2.05 g, 4.05 mmol/g of solid) was dissolved in anhydrous THF (25 mL) and this mixture was added to the solid/rhodamine B suspension and then stirred for 6 h at room temperature in an argon atmosphere. **S1** particles were isolated as a red solid, washed with H_2O and EtOH, and finally dried in a vacuum for 24 h.

2.3.5. *Synthesis of S2.* Solid **S0** (1 g) was suspended in 40 mL of THF/hydrocortisone solution (296 mg, 0.8 mmol/g of solid) under argon. Suspension was stirred at room temperature overnight. Next, compound **1** (2.05 g, 4.05 mmol/g of solid) was dissolved in anhydrous THF (25 mL) and was then added to the solid/hydrocortisone suspension. The obtained suspension was stirred under argon and at room temperature during 6 h. **S2** particles were isolated as a yellow solid, washed with EtOH and H_2O, and finally dried for 24 h in a vacuum.

2.4. Controlled release studies. The controlled release behavior of solids **S1** and **S2** at pH values found along the gastrointestinal tract (GIT) (2.0, 4.5 and 7.4) and in the presence of a chemical reducing agent (sodium dithionite), to simulate the azo-reductive environment, were assessed. For this purpose, corresponding solid (2 mg) was suspended in 2 mL of the aqueous solution at the selected pH. Aliquots were taken at scheduled times up to 24 h and centrifuged

to discard the solid before analyzing. The controlled release performances of both solids were tested under *in vitro* digestion conditions using simulated solutions for GIT fluids including saliva, gastric juice, duodenal juice, bile and colon (in which azoreductor agent sodium dithionite was added for colon reducing environment simulation). *In vitro* digestion assays were performed with 2 mg of solid **S1** or **S2** at 37 ^{o}C (simulating the body temperature in humans) and shaken (100 rpm) to obtain homogeneous suspensions of microparticles. Digestions started by the addition of 320 µL of simulated saliva fluid (pH = 6.8 ± 0.1) and incubating during 5 min. Next, 630 µL of simulated gastric juice was added and the mixture was stirred 2 h (total volume of 950 µL and pH = 1.3 ± 0.2). Then, 630 µL of simulated duodenal juice, 320 µL of bile and 100 µL of a bicarbonate solution (1 M) were added simultaneously (total volume of 2 mL and pH = 6.0 ± 0.5). The resulting solution was stirred during 2 h. Finally, colon fluid was simulated with the addition of 2 mg/mL of sodium dithionite to the last mixture (total volume of 2 mL pH = 6.0 ± 0.5). Aliquots were collected at scheduled times up to 28 h (4 h approximately to reach the colon, plus 24 h of colon residence time), centrifuged, and analyzed. In order to determine the amount of cargo delivered from **S1** microparticles, supernatants were loaded into 96-well plate and then the rhodamine B emission at 572 nm (upon excitation at 555 nm) was measured. The amount of hydrocortisone released from **S2** microparticles was assessed from the supernatants using an HPLC. The released 5-ASA was also analyzed by HPLC (*vide infra*).

2.5. 5-ASA and hydrocortisone quantification. HPLC (with a reverse-phase column) was used for 5-ASA and hydrocortisone determination using the methods described by Lunn[40] and Navarro.[41] The HPLC equipment used was a Hitachi LaChrom Elite liquid chromatograph connected to an auto-sampler and a UV detector (L-2200 and L-2400, respectively). For both analytes, a C18 column (Kromaphase 100 of 150 mm × 4.6 mm i.d., 5 µm particle size) was used for separations. For the 5-ASA determinations, mobile phase: (A) 50 mM sodium phosphate / (B) methanol, isocratic program: 90% A / 10% B for 15 min. The wavelength of the UV detector was set at 365 nm. For hydrocortisone determinations, mobile phase: (A) water / (B) acetonitrile, isocratic program: 70% A / 30% B for 15 min. The UV wavelength of the UV detector was set at 245 nm. Both analytes were quantified using a calibration curve (peak area vs. analyte concentration). The used method was validated using a recovery study. At this respect, simulated GIT fluids were spiked with both analytes (5-ASA or hydrocortisone) at five

different concentrations. The recovery values were estimated from the determined concentration vs. the amounts of 5-ASA or hydrocortisone added. All the recovery values were near to 100%.

2.6. *In vivo* studies. These studies followed the Principles of Laboratory Animal Care and were approved by the Institutional Ethics Committee of the University of Valencia (according to RD 1201/2005). For the *in vivo* studies male Wistar rats (aged 8-12 weeks and with an weight in the 270-330 g interval) were used. Animals were housed in an air-conditioned room (12 h light/dark cycles, 22 ± 3 ºC, 55 ± 5% humidity) and were allowed free access to laboratory chow and water during all the time of the studies.

2.6.1. *In vivo* pharmacokinetic studies. In a first step, male Wistar rats (with an average weight of 300±30 g) were anesthetized to facilitate the cannula implantation 24 h before the experiment. Then, in a second step, a previously reported method for jugular vein permanent cannulation was followed.[42] The implanted cannula allowed blood sampling. The animals were randomly ascribed (n= 8-10) to different groups: Group 1: 1 mL of rhodamine B solution (750 µg/mL in saline solution) was given orally. Group 2: 1.75 mL of a **S1** suspension (containing 30 mg of solid which should deliver about 750 µg of rhodamine B) was given orally. Blood samples (0.6-0.7 mL) were drawn with heparinized syringes and replaced by heparinized saline (10 IU/mL), at previously established sampling time (up to 4 h). Plasma samples were centrifuged (10,000 rpm, 10 min) and supernatant was stored at -20 °C until analyzed by HPLC. A fluorescence detector, with excitation and emission wavelength fixed at 225 and 535 nm respectively, was used. The solvent delivery system (Alliance System, Waters 2695) was used to provide a mobile phase 70:30 v/v of trifluoroacetic acid aqueous solution (pH 3)-acetonitrile. The stationary phase was a Waters model Nova Pak C-18 (150 mm length, 3.9 mm in diameter and particle size of 4 µm) column preceded by a Teknocroma TCR-C130-B pre-column. Flow rate was set at 1 mL/min and the injection volume was 90 µL for *in vivo* samples. Retention time of rhodamine B was 2.5 min. Analytical method was validated in terms of selectivity, specificity, precision, linearity and accuracy. After 4 h, rat subjects were euthanized and the cecum, colon tissues and feces were extracted and treated in order to determine rhodamine B amount. The analyzed rhodamine B corresponded to that released from **S1** particles in the GIT of subjects (**S1** release was not forced *in vitro*).

2.6.2. *In vivo* efficacy studies.

2.6.2.1. Inducing colonic inflammation. Several slight modifications were introduced in the method described by C. Mura et al. to induce the chronic inflammation model in colon rat.[43] For this purpose, rats were indistinctly separated in different treatment groups (having free access to water) and were then anaesthetized with isoflurane. TNBS solution in 59% v/v ethanol (0.6 mL, 78 mg/kg body weight) was instilled into the lumen of the colon using a graduated rubber cannula inserted rectally into the colon (taking into account that the tip was 8 cm proximal to the anus). After the induction procedure, the development of inflammation was monitored daily for the next 10 days that the assays lasted. Rats were sacrificed using an overdose of isoflurane at the end of the 10th day (after induction with TNBS). Inflammation development was evaluated through determination of the clinical activity score, colon/body weight ratio and also studying changes in tissue histology.

2.6.2.2. Treatment study design. Rats were distributed into four groups: Group 1 (positive control group, 3 rats) with saline solution as treatment; Group 2 (8 rats) treated with a suspension of **S0** (empty mesoporous silica microparticles); Group 3 (8 rats) treated with hydrocortisone solution; Group 4 (8 rats) treated with an aqueous suspension of **S2** microparticles. The hydrocortisone dose that groups 3 and 4 received (5.58 mg/kg/day) was calculated from the dose normally used for humans.[44] All the treatments were carried out using an oral gavage once a day during 3 days in the most intensive inflammation period (days 3, 4 and 5 after TNBS administration). Groups and treatment are summarized in Table 1.

Table 1. Treatment groups.

Group 1	Group 2	Group 3	Group 4
saline solution (1.5 mL)	60 mg of **S0** in 1.5 mL	1.5 mg hydrocortisone in 1.5 mL	30 mg **S2** in 1.5 mL

2.6.2.3. Clinical activity score system. A clinical score that assessed weight loss, stool consistency and rectal bleeding (see Table 2) was used to quantify colitis activity.[27,45]

Table 2. Clinical activity score system.

CONTROL	RANGE	SCORE
% WEIGHT LOSS	<1%	0
	1-5%	1
	5-10%	2
	10-20%	3
	>20%	4
STOOL CONSISTENCY	Well-formed pellets	0
	Pasty and semi-formed stools	2
	Liquid stools or absence	4
BLEEDING	No blood	0
	Positive finding	2
	Gross bleeding	4

The sum of these scores resulted in the clinical activity which ranged from 0 (healthy animal) to 12 (higher colitis activity). An activity score of 12 was assigned to rats that died or had to be sacrificed before day 10.

2.6.2.4. Assessing colonic injury and inflammation. Rats were monitored during the 10 days period of the assay and, finally, the clinical activity score of colitis was evaluated. On day 10 after administering TNBS, rats were sacrificed with isoflurane to obtain the distal colon for subsequent processing and analyzing. The samples from inflamed tissue were excised to calculate C/B ratio, being C the distal colon weight, and B the body weight. Besides, an histological evaluation was also carried out.

2.6.2.5. Determining the colon/body weight ratio. After animal scarification, the distal colon was extracted and longitudinally opened along the mesenteric edge. Then, colon was washed with a 0.9% (w/v) saline solution, weighted and placed on a glass plate with the mucosal surface lying upward.[46] The 8 cm segment distal colon weight ratio was calculated as an index of colonic tissue edema.

2.6.2.6. Histological evaluation. A 3 cm sample from distal colon (and a similar portion from proximal part) were excised from each subject and maintained in 4% (v/v) *p*-formaldehyde for 24 h. Afterward, samples were changed to a 0.4% (v/v) *p*-formaldehyde medium in order to perform the microscopic studies. These colonic tissue samples were routinely processed and then embedded in paraffin. Then, longitudinal sections of 5 µm were stained with eosin and hematoxylin. Microscopic assessment by light microscope was performed blind on coded slices.

2.6.2.7. Statistical analysis. Non-parametric U-Mann-Whitney and Kruskal-Wallis tests were performed to assess the differences among groups using SPSS v.22.0 (SPSS Inc., USA) on Windows.

3. RESULTS AND DISCUSSION

3.1. Synthesis of mesoporous silica microparticles functionalized with molecular gates. The mesoporous silica carrier was synthesized following previously reported procedures with minor adjustments.[39] In this synthetic protocol, tetraethylorthosilicate (TEOS) was employed as the source of silica and 1-hexadecyltrimethylammonium bromide (CTABr) as a structure directing agent. The resulting white powder was rinsed and then calcined (in order to remove the CTABr template). This protocol yielded the mesoporous silica microparticles **S0**. Pores in **S0** where loaded with a selected dye (rhodamine B) or hydrocortisone and then the external surface of both microparticles was functionalized with the olsalazine derivative **1**. This procedure yielded the final solids **S1** (loaded with rhodamine B) and **S2** (containing hydrocortisone) as depicted in Scheme 1. The pores of **S1** and **S2** were expected to be capped due to the presence of bulky azoderivative **1** anchored to the external surface of microparticles. Besides, rhodamine B or hydrocortisone release should be observed in the presence of azoreductor agents such as azoreductase enzymes, produced by colon bacteria, or chemical reducing species.

The synthesis of azo derivative containing trialkoxysilane moieties (**1**) was carried out using a two-step sequence (see Scheme 2). First olsalazine sodium salt was protonated to yield the free acid (**1a**), which was then reacted with (3-aminopropyl) triethoxysilane (**1b**). The final azo

compound containing alkoxysilane groups (**1**) was fully characterized using ^{1}H and ^{13}C-NMR and HRMS.

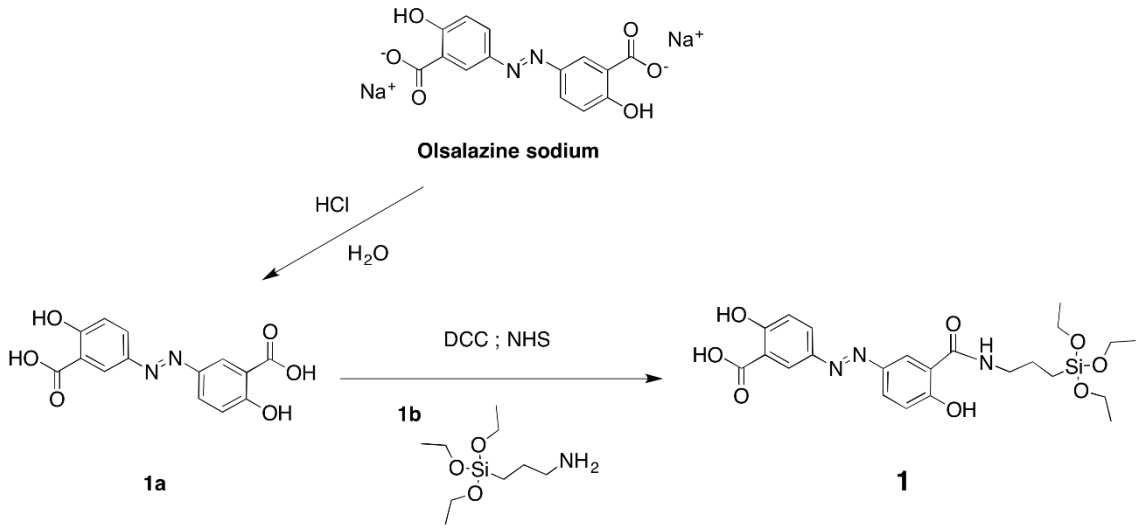

Scheme 2. Synthetic route used to prepare **1**.

3.2. Characterization of the final materials. Solids **S0, S1** and **S2** were characterized using powder X-ray diffraction (PXRD), transmission electron microscopy (TEM), thermogravimetric measurements (TGA), and N_2 adsorption-desorption isotherms. The PXRD pattern of the as-synthesized microparticles showed four reflections indexed as (100), (110), (200) and (210) Bragg peaks typical of a mesoporous material with a hexagonal order. A marked shift of the (100) reflexion in calcined material **S0** was observed. This shift was ascribed to silanol groups condensation during the calcination step. Moreover, the preservation of the (100) reflection in the PXRD patterns of **S1** and **S2** microparticles showed that the mesoporous structure was preserved during the loading process and functionalization with **1**. TEM images of **S0** and **S2** also showed the typical porosity of mesoporous silica materials, which confirmed that there was no framework modification (data not shown).

The N_2 adsorption-desorption measurements on the calcined solid (**S0**) showed a type IV isotherm, typical of the mesoporous silica materials. This isotherm presented at intermediate P/P_0 values (0.2-0.4) an adsorption step. From the adsorption branch of the isotherm the values of pore volume (0.98 $cm^3\ g^{-1}$) and pore diameter (2.55 nm) were calculated. Besides, the pore

diameter estimated from the TEM images agreed with this calculated value. The total specific surface of **S0** microparticles (1193 m^2 g^{-1}) was evaluated using the Brunauer–Emmett–Teller (BET) model. On the other hand, the N_2 adsorption-desorption isotherms of **S1** and **S2** microparticles were typical of mesoporous systems with partially filled mesopores. When compared with **S0**, both, the specific surface area and adsorbed N_2 volume were clearly reduced (see Table 3). The loading of pores with rhodamine B (for **S1**) or hydrocortisone (for **S2**), and the grafting of olsalazine derivative **1** onto the external surface accounted for the reduction in the BET surface observed for both solids.

Table 3. Structural parameters for **S0**, **S1** and **S2** microparticles.

	S_{BET} (m^2 g^{-1})	pore volume[a] (cm^3 g^{-1})	pore size[a,b] (nm)
S0	1193	0.98	2.55
S1	200	0.06	-
S2	770	0.35	-

[a] Total pore volume estimated using the BJH model.

[b] Pore size according to the BJH model applied to the adsorption branch of the isotherm (for $P/P_0 < 0.6$) which can be assigned to the mesopores generated by the surfactant.

Table 4. Total organic matter (in g) content per gram of SiO_2, olsalazine derivative **1** (in g) content per gram of SiO_2, dye or drug (hydrocortisone: HC) released (in µg) per mg of solid and drug (5-ASA) released per mg of solid for **S1** and **S2**.

solid	organic content (g/g SiO_2)	**1** (g/g SiO_2)	dye/HC release (µg/mg solid)	5-ASA release (µg/mg solid)
S1	0.24	0.16	21.50	107
S2	0.19	0.11	24.36	93

Thermogravimetric analysis and ^{1}H NMR measurements were employed to assess the organic content in **S1** and **S2** (see Table 4). The amount of total organic matter was larger in **S1** than in **S2**, which agrees with the larger specific surface found for **S2** (see Table 3), indicating that the loading of the mesoporous support with rhodamine B in **S1** was more efficient than for hydrocortisone in **S2**. The amounts of olsalazine derivative grafted onto the outer surface of **S1** and **S2** were determined by ^{1}H NMR measurements. For this purpose, the corresponding solid

was dissolved in NaOD/D_2O using $(CH_3CH_2)_4NBr$ as internal standard. Moreover, HPLC was used to quantify the amount of 5-ASA released. In the presence of a reducing agent (*vide infra*) **S1** and **S2** were able to deliver 107 µg/mg and 93 µg/mg of 5-ASA, respectively. FT-IR analysis on **S2** revealed the presence of typical amide signals at 1633 cm^{-1} (carbonyl), 1594 cm^{-1} (N-H torsion) and 1486 cm^{-1} (C-N stretching), and azo signal at 1558 cm^{-1} (data not shown).

3.3. Payload delivery from S1 and S2. The cargo release (rhodamine B or hydrocortisone) from solids **S1** and **S2** was evaluated at acidic pH (2.0 and 4.5) and at neutral pH (7.4) in the absence of in the presence of sodium dithionite (an azoreductor agent). These pH values were selected bearing in mind typical pH values for gastric juices (pH 2.0), transition from stomach to the intestine (pH 4.5) and intestine (pH 7.4). Cargo release profiles for **S1** and **S2** microparticles are shown in Figure 1a and 1b, respectively. Aqueous suspensions of **S1** and **S2** showed poor rhodamine B (**S1**) or hydrocortisone (**S2**) release at acidic and neutral pHs. However, a marked delivery of the entrapped payload (rhodamine B from **S1** and hydrocortisone from **S2**) was seen at pH 7.4 when sodium dithionite was present, which showed a sustained release profile that reached ca. 90% (for **S1**) and 80% (for **S2**) of the maximum dye/drug delivered after 6 h. The observed cargo release was ascribed to the presence of the azoreductor agent (sodium dithionite), which is able to reduce the azo groups in the capping molecule **1**. This azo group reduction resulted in pore opening and rhodamine B (**S1**) or hydrocortisone (**S2**) release. The maximum rhodamine B release from **S1** was ca. 21.50 µg/mg solid, in the presence of an azoreductor (pH = 7.4). Under the same experimental conditions, the maximum hydrocortisone release from **S2** was ca. 24.36 µg/mg solid. The release of 5-ASA in the absence of the azoreductor agent was negligible (at pH of 2.0, 4.5 and 7.4), although a clear cargo release was attained after 1 h for **S1** and **S2**, respectively, when sodium dithionite was present. To conclude, both pharmaceutical active compounds (i.e. hydrocortisone and 5-ASA) were released at a neutral pH when the reducing agent sodium dithionite was present, mimicking the colon environment.

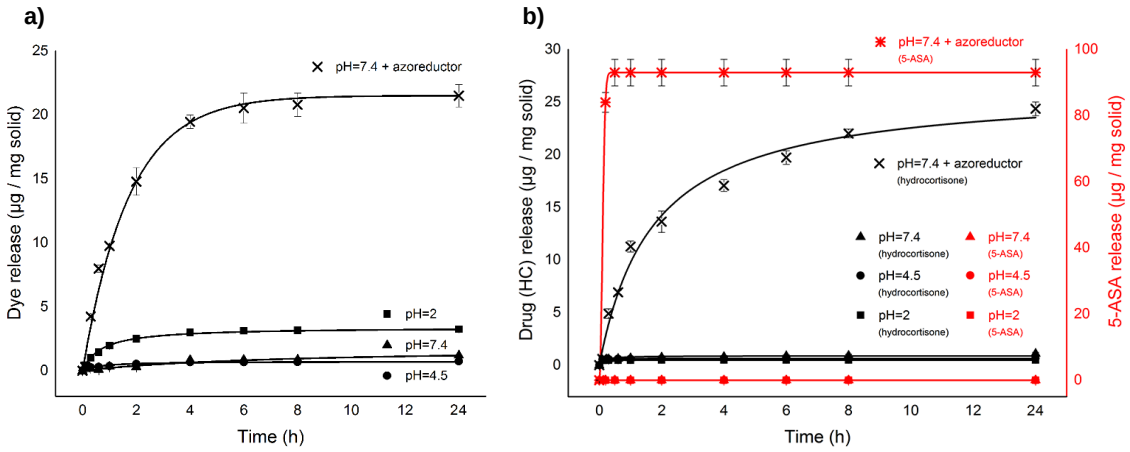

Figure 1. (a) Release profiles of rhodamine B from **S1** microparticles in water at pH ≈ 2 (square), pH ≈ 4.5 (circle), pH ≈ 7.4 (triangle) and pH ≈ 7.4 in the presence of sodium dithionite (2 mg/mL) (cross). (b) Release kinetics of hydrocortisone (black) and 5-ASA (red) from **S2** microparticles in water at pH ≈ 2 (square), pH ≈ 4.5 (circle), pH ≈ 7.4 (triangle) and pH ≈ 7.4 in the presence of sodium dithionite (2 mg/mL) (cross: hydrocortisone, star: 5-ASA).

3.4. *In vitro* digestion model assay. In a further step the delivery of olsalazine and 5-ASA from **S2** was thoroughly evaluated in a digestion model using simulated solutions. The used model was inspired in that reported by Oomen, and consisted in a procedure of three steps simulating the digestive process (from the mouth, through the stomach, and to the small intestine).[47,48] Moreover, we added an additional step after the small intestine, in order to simulate digestion at colonic area. In a typical experiment, **S2** (2 mg) was suspended for 5 min in the simulated saliva at 37.5 ^{o}C, afterwards simulated gastric juice (stomach) was added and the suspension was stirred during 2 h. Next, the simulated small intestine fluid (duodenal simulated juice, bile and bicarbonate solution) was added and the mixture was stirred for 2 h. Finally, addition of sodium dithionite simulated the azoreductor colon environment. This final suspension was left for 24 h. The release of hydrocortisone and 5-ASA from **S2** was quantified by HPLC under the conditions described above. Figure 2 shows the obtained results.

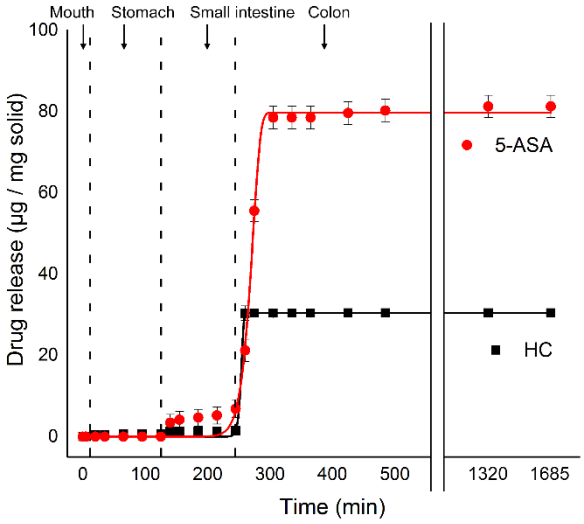

Figure 2. Release kinetics of the hydrocortisone (HC) and 5-ASA from **S2** in simulated GIT fluids.

As seen in Figure 2, the released hydrocortisone or 5-ASA from **S2** was less than 5% in the simulated mouth, stomach and small intestine juices, which indicates that acidic media over a period shorter than 2 h does not induce hydrocortisone or 5-ASA delivery. In contrast, a clear release of both drugs (maximum delivery was 30.44 and 81.25 µg/mg solid for hydrocortisone and 5-ASA respectively) was observed when **S2** came into contact with the simulated colon juice due to the reduction of the azo linkages in the gated material.

3.5. *In vivo* pharmacokinetic studies. To test both the specific colon release and systemic absorption prevention, *in vivo* pharmacokinetic studies with **S1** microparticles were performed. Rats in group 1, which were administered with a rhodamine B solution, showed plasma levels of rhodamine B with a maximum of 0.45 µg/mL 1 h after administration (Figure 3). Group 2, which received formulation **S1**, showed negligible rhodamine B systemic absorption and no rhodamine B was found in plasma (Figure 3). The presence of rhodamine B in the cecum, colon and feces was also evaluated. Figure 4 shows significant larger presence of rhodamine B in the colon and cecum in rats fed with **S1** (Group 2) compared with those treated with rhodamine B (Group 1). These results evidence the specific dye/drug delivery to the colon from the systems designed in this work, and also demonstrated that systemic absorption was avoided when rhodamine B was

encapsulated in **S1**. Besides, C_{max} and T_{max} values for rats in groups 1 (administered with rhodamine B solution) and 2 (treated with **S1**) are shown in Table 5.

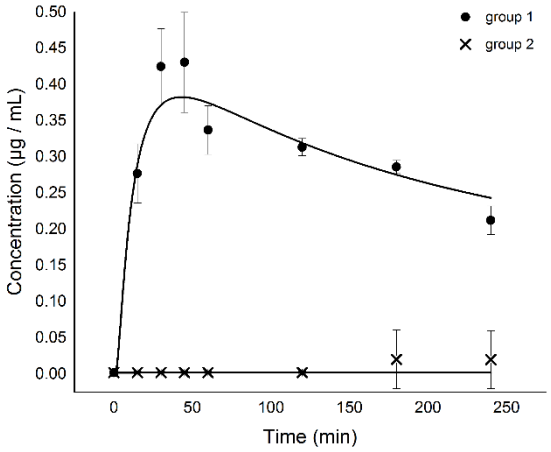

Figure 3. The rhodamine B concentration (µg/mL) in plasma. For the subjects which received rhodamine B solution (Group 1) and those which receiving suspension **S1** (Group 2).

Table 5. C_{max} and T_{max} of both formulations assayed. (n = 4).

	AUC t_0-t_∞/Dose (mL^{-1} h^{-1})	C_{max} (µg/mL)	T_{max} (min)
Group 1	56.92	0.45*	50*
Group 2	9.21	0.02	250

Note: * statistically significant differences ($p < 0.05$) between Group 1 and Group 2

C_{max} (maximal drug concentration), T_{max} (time to reach C_{max}) of rhodamine B plasma profiles were calculated and compared to determine if the prepared suspension modify the dye solution parameters. Presented results are the average of four animals per group.

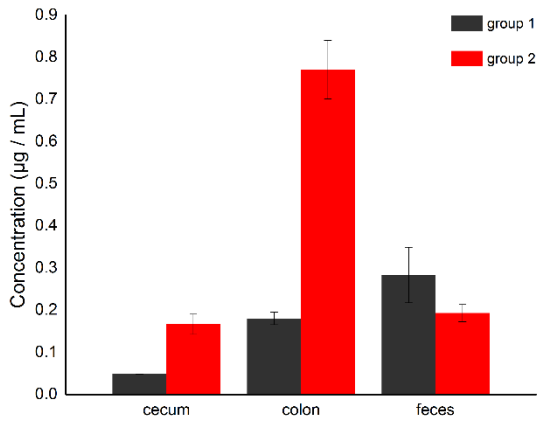

Figure 4. Rhodamine B concentration (µg/mL) in the cecum, colon and feces. For the subjects that received rhodamine B solution (Group 1) and those administered **S1** suspension (Group 2).

3.6. *In vivo* efficacy studies

3.6.1. Inducing colonic inflammation. TNBS was used to induce the IBD model in rats. In this model, enema administration of TNBS (50% V/V in ethanol) induced IBD-like injuries. The reproducibility, simplicity dose- and time-related development of inflammation are the most remarkable advantages of this model.[49,50] Inflammation development was monitored daily. During the period of study, individuals suffered weight loss and diarrhoea, but no rectal bleeding.

Figure 5A shows the typical appearance of a healthy colon of rats. Figure 5B shows the opened colon of the rats that received saline serum (placebo treatment, Group 1), whereas Figures 5C to E show the opened colons of rats after inducing colitis with TNBS and treated with **S0**, hydrocortisone and **S2**, Groups 2, 3 and 4 respectively. All rats were sacrificed 10 days after treatment with TNBS. Colons from Groups 1 (Figure 5B) and 2 (Figure 5C) were strikingly similar and both presented a thick rigid bowel and showed necrotic tissue. In colons from individuals treated with hydrocortisone (Group 3, Figure 5D) some tissue started to heal, but although thickened tissue and necrotic zone had reduced, they were still present. In contrast, colons of rats from Group 4 treated with **S2** (Figure 5E) generally appeared healthy, and only a few presented very small mild injuries. In addition, after the administration of **S2**, subjects from Group 4 gained some weight and presented normal stools, similar to some subjects of Group 3 (which received hydrocortisone solution). On the other hand, after the administration of saline solution or **S0**, rats from Groups 1 and 2 had diarrhea and lost weight throughout the experiment. Figures 6 and 7 showed the effects after oral administration of the different formulations on the clinical activity score and the colon/body weight, respectively.

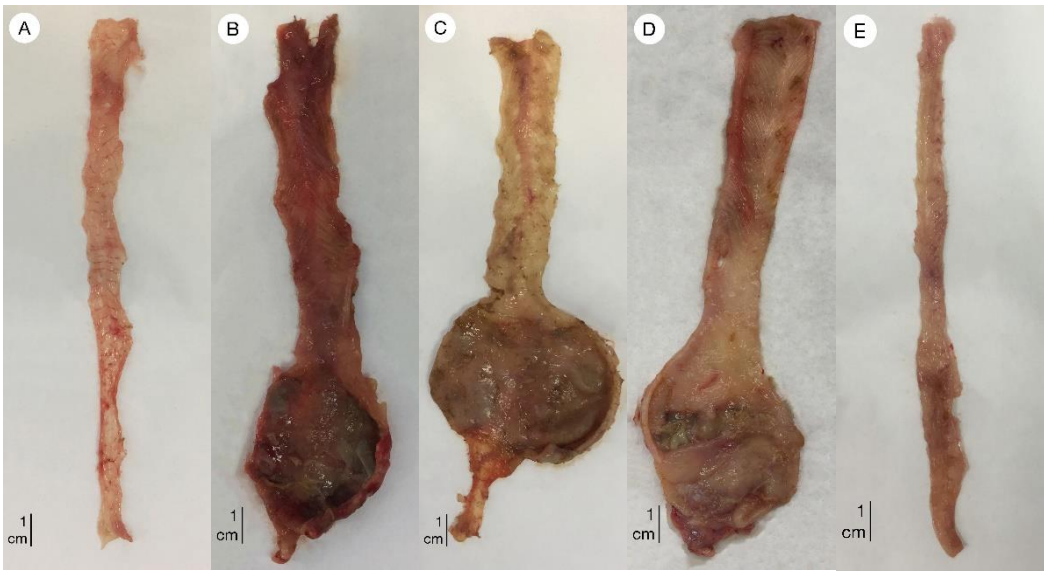

Figure 5. Pictures of rat colon 10 days after inducing colitis with TNBS: **A** healthy control (without TNBS administration), **B** positive control (Group 1, treated with saline serum), **C** (Group 2, treated with **S0**), **D** (Group 3, administered with hydrocortisone) and **E** (Group 4, administered with **S2**).

The colon/body weight ratio decreased considerably in rats of Group 4 (treated with **S2**) compared to the control, which received saline solution (Group 1). In contrast no accentuated effect was observed on the colon/body weight ratio for subjects treated with **S0** particles (Group 2). Rats in Group 3 (treated with the hydrocortisone solution) had a wide variability, with several cases of improvement and several cases without improvement at all (Figure 6). Similar results (i.e. wide variability) were found for Group 3 in the clinical activity score (Figure 7). This large variation observed for Group 3 can be due to one of the following reasons: a) orally taken hydrocortisone is almost absorbed completely before reaching its site of action; b) the dose of an administered drug in not enough to allow recovery. In contrast, the **S2** formulation allowed the release of two drugs, i.e. hydrocortisone (carried inside the mesoporous silica microparticles) and 5-ASA (externally anchored to the surface of microparticles), which results in a high concentration of both active ingredients in the injured area having a remarkable therapeutic effect.

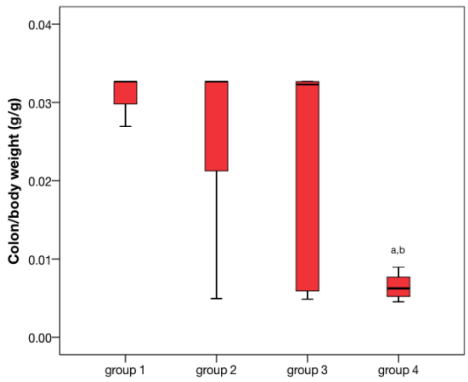

Figure 6. The colon/body weight ratio of rats with TNBS-induced colitis after receiving subsequent treatments: saline solution (Group 1, positive control), **S0** (Group 2), hydrocortisone (Group 3) and **S2** (Group 4). In each box represents the median value, the 25% and 75% percentiles, the minimal and maximal values (^{a,b} statistical significant difference ($P < 0.05$) compared to the saline and **S0** solid, respectively).

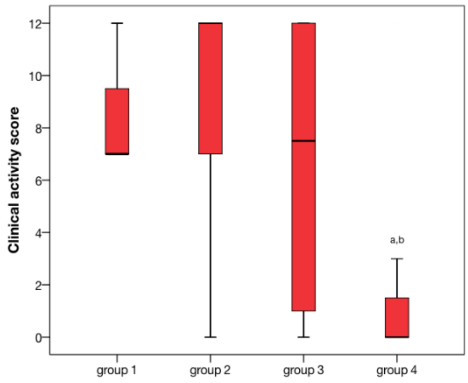

Figure 7. The clinical activity score of rats with TNBS-induced colitis after receiving subsequent treatments: saline solution (Group 1, positive control), **S0** (Group 2), hydrocortisone (Group 3) and **S2** (Group 4). In each box represents the median value, the 25% and 75% percentiles, the minimal and maximal values (^{a,b} statistical significant difference ($P < 0.05$) compared to the saline and **S0** solid, respectively).

3.6.2. Histological evaluation. Histological tissue examinations in a healthy control rats, and in rats treated with TNBS of different groups: i.e. 1 (saline solution, positive control group); 2 (**S0**); 3 (hydrocortisone solution); 4 (**S2** formulation) were carried out. Samples were always taken from the sacrificed subjects on day 10 after TNBS treatment. The healthy control showed a

usual colon structure: i.e. connective tissue and goblet cells (lamina propria, Figure 8A), healthy mucosa with enterocytes, muscularis mucosae, normal submucosa and muscularis externa. On the other hand, tissues from rats of Groups 1 and 2 showed loss of necrotic mucosa and substitution for granulation tissue (see Figure 8B and 8C). Besides, a strong inflammatory process was present in the lamina propria, submucosa and muscularis extern in the individuals of both groups. Figure 8B and 8C also show the ulceration process with the fibrinoid necrosis of the mucosal surface and granulation tissue below necrotic tissue. Rats of Group 3 (treated with hydrocortisone) only showed superficial erosion, thinning mucosa (complemented by a thickening of muscularis mucosae), and a chronic inflammatory process which affected the mucosa and submucosa with an early development of lymphoid follicle. Besides, Figure 8D also shows a small number of parts with a normal mucosa structure. However, the presence of strong follicular hyperplasia (in the muscularis externa and parts with necrosis), loss of mucosa and substitution for granulation tissue, and the inflammation process is also observed in Figure 8D. The individuals treated with **S2** microparticles (Group 4) showed a normal mucosal structure with the presence of minor chronic inflammation in muscularis propria (see Figure 8E).

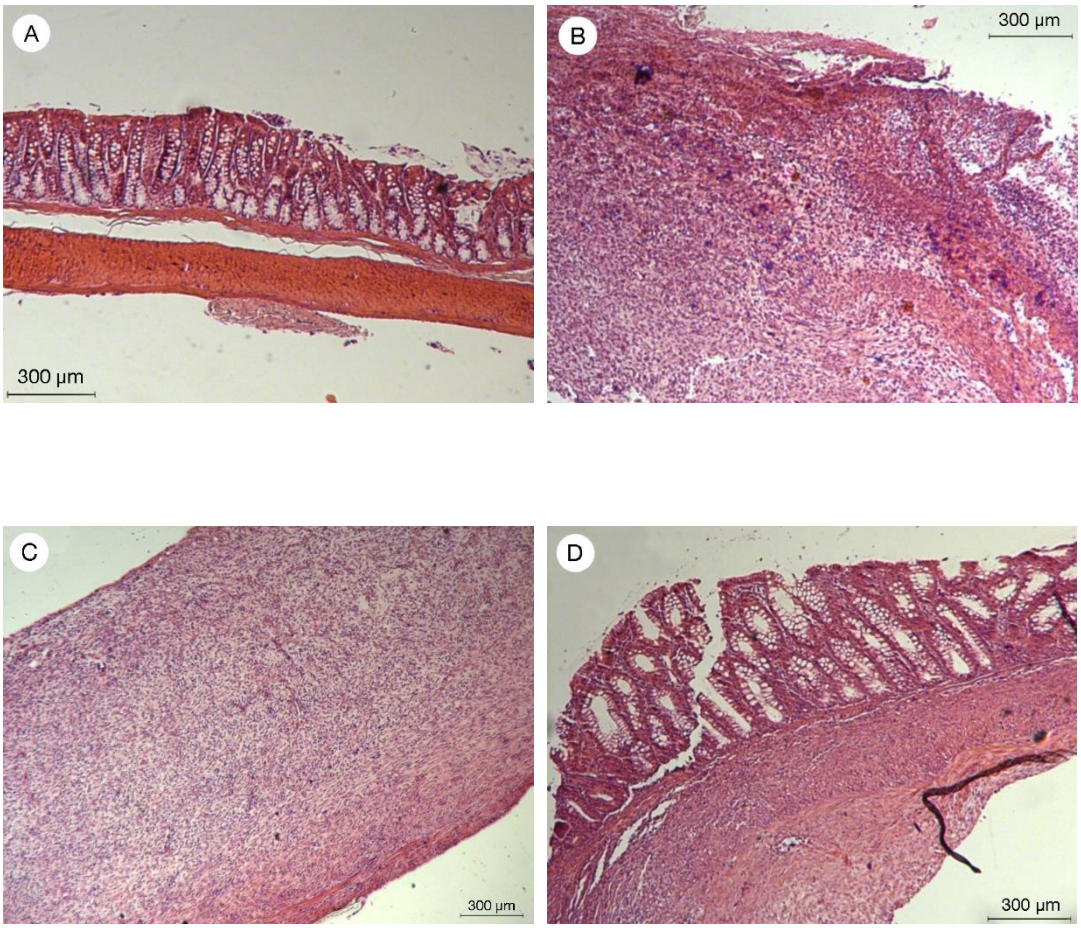

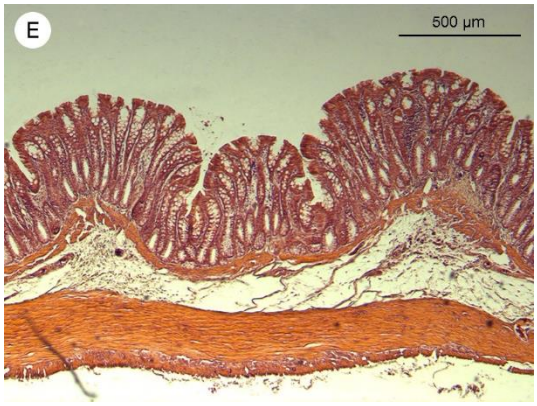

Figure 8. Histology of a representative colon specimen of healthy rats (A) and rats after inducing colitis with TNBS, treated and sacrificed on day 10: (B) administered with saline solution (positive control, Group 1), (C) treated with **S0** (Group 2), (D) administered with hydrocortisone (Group 3) and (E) treated with **S2** (Group 4).

The histological findings indicated that Group 1 individuals (the saline-treated TNBS group) showed necrosis, strong inflammation and mucosa loss. Similar results were observed with the rats treated with microparticles **S0** (Group 2). In contrast, the histological findings of the rats treated with **S2** (Group 4) showed an intensive regeneration, softer inflammation, and an almost normal mucosal structure. The information obtained by the colon/body weight ratio, the clinical activity score and the histological evaluation, confirming the usefulness of **S2** system to treat IBD. Moreover, it can be stated that our formulation improved the results reported in previous studies by C.Mura et al., M. Naeem et al. or A. H. Teruel et al., with the added benefit of not involving any systemic intervention.[29,43,51]

4. CONCLUSIONS

A novel oral colon drug delivery system is designed and prepared, and its efficiency to treat IBD was evaluated *in vivo* in a TNBS-induced colitis rat model. The prepared system consists of mesoporous silica microparticles loaded with either, rhodamine B (**S1**) or hydrocortisone (**S2**),

and decorated on the external surface with an olsalazine derivative. This olsalazine derivative is a bulky azo compound, covalently grafted onto the external surface of the loaded support through amide linkages, which yielded drug 5-ASA upon hydrolysis of the azo bonds. Both materials (i.e. **S1** and **S2**) remained capped at neutral an acidic pH, yet a remarkable payload delivery is evident when sodium dithionite (a reducing agent that mimics the azo-reductase enzymes present in colon) was present. Cargo release is a consequence of the sodium dithionite-induced reduction of azo bonds in the bulky capping ensemble, whereas 5-ASA is also delivered from both microdevices upon the hydrolysis of the olsalazine derivative. *In vivo* pharmacokinetic studies performed with **S1** showed specific rhodamine B delivery at colonic area. The clinical activity score, the colon/body weight ratio and the histological colon tissue evaluation evidenced that rats with chronic colon inflammation and treated with microparticles **S2** show an improvement in the pathology due to the simultaneous hydrocortisone and 5-ASA release. In conclusion, we demonstrate that microparticles reported here can be used to release drugs specifically in the last intestine part, while diminishing systemic absorption. Specifically **S2** is a formulation able to treat IBD due to the double drug delivery (i.e. hydrocortisone and 5-ASA release) at the colon.

5. ACKNOWLEDGEMENTS

We thank the Generalitat Valenciana (Project PROMETEO2018/024) and the Spanish Government (Projects AGL2015-70235-C2-2-R and MAT2015-64139-C4-1-R (MINECO/FEDER)) for support. AHT thanks the Spanish MEC for his FPU fellowship. The authors also thank the support of the Electron Microscopy Service at the UPV. The SCSIE (of the Universitat de València) is also gratefully acknowledged for all the equipment used. NMR spectra were measured at the U26 facility of ICTS “NANBIOSIS” at the Universitat de València.

6. REFERENCES

(1) Baumgart, D.; Sandborn, W. Crohn’s Disease. *Lancet* **2012**, *380*, 1590–1605.

(2) Liu, T.-C.; Stappenbeck, T. S. Genetics and Pathogenesis of Inflammatory Bowel Disease. *Annu. Rev. Pathol.* **2016**, *11*, 126-148.

(3) Pierik, M.; Yang, H.; Barmada, M. M.; Cavanaugh, J. A.; Annese, V.; Brant, S. R.; Cho, J. H.; Duerr, R. H.; Hugot, J. P.; McGovern, D. P.; Paavola-Sakki, P.; Radford-Smith G. L.; Pavli, P.; Silverberg, M. S.; Schreiber, S.; Taylor, K. D.; Vlietinck, R. The IBD International Genetics Consortium Provides Further Evidence for Linkage to IBD4 and Shows Gene-Environment Interaction. *Inflamm. Bowel Dis.* **2005**, *11*, 1–7.

(4) Loftus, E. V. Clinical Epidemiology of Inflammatory Bowel Disease: Incidence, Prevalence, and Environmental Influences. *Gastroenterology* **2004**, 1504–1517.

(5) Ye, Y.; Pang, Z.; Chen, W.; Ju, S.; Zhou, C. The Epidemiology and Risk Factors of Inflammatory Bowel Disease. *Int. J. Clin. Exp. Med.* **2015**, *8*, 22529–22542.

(6) Lupp, C.; Robertson, M. L.; Wickham, M. E.; Sekirov, I.; Champion, O. L.; Gaynor, E. C.; Finlay, B. B. Host-Mediated Inflammation Disrupts the Intestinal Microbiota and Promotes the Overgrowth of Enterobacteriaceae. *Cell Host Microbe* **2007**, *2*, 119–129.

(7) Takaishi, H.; Matsuki, T.; Nakazawa, A.; Takada, T.; Kado, S.; Asahara, T.; Kamada, N.; Sakuraba, A.; Yajima, T.; Higuchi, H.; Inoue, N.; Ogata, H.; Iwao, Y.; Nomoto, K.; Tanaka, R.; Hibi, T. Imbalance in Intestinal Microflora Constitution Could Be Involved in the Pathogenesis of Inflammatory Bowel Disease. *Int. J. Med. Microbiol.* **2008**, *298*, 463–472.

(8) Sokol, H.; Seksik, P.; Furet, J. P.; Firmesse, O.; Nion-Larmurier, I.; Beaugerie, L.; Cosnes, J.; Corthier, G.; Marteau, P.; Doraé, J. Low Counts of Faecalibacterium Prausnitzii in Colitis Microbiota. *Inflamm. Bowel Dis.* **2009**, *15*, 1183–1189.

(9) Friswell, M.; Campbell, B.; Rhodes, J. The Role of Bacteria in the Pathogenesis of Inflammatory Bowel Disease. *Gut Liver* **2010**, *4*, 295–306.

(10) Qiu, X.; Zhang, M.; Yang, X.; Hong, N.; Yu, C. Faecalibacterium Prausnitzii Upregulates Regulatory T Cells and Anti-Inflammatory Cytokines in Treating TNBS-Induced Colitis. *J. Crohn's Colitis* **2013**, *7*, 558-568.

(11) Yu, C. G.; Huang, Q. Recent Progress on the Role of Gut Microbiota in the Pathogenesis of Inflammatory Bowel Disease. *J. Dig. Dis.* **2013**, *14*, 513–517.

(12) Kappelman, M. D.; Rifas-Shiman, S. L.; Porter, C. Q.; Ollendorf, D. A.; Sandler, R. S.;

Galanko, J. A.; Finkelstein, J. A. Direct Health Care Costs of Crohn's Disease and Ulcerative Colitis in US Children and Adults. *Gastroenterology* **2008**, *135*, 1907–1913.

(13) Kappelman, M. D.; Rifas-Shiman, S. L.; Porter, C. Q.; Ollendorf, D. A.; Sandler, R. S.; Galanko, J. A.; Finkelstein, J. A. Direct Health Care Costs of Crohn's Disease and Ulcerative Colitis in US Children and Adults. *Gastroenterology* **2008**, *135*, 1907–1913.

(14) Rocchi, A.; Benchimol, E. I.; Bernstein, C. N.; Bitton, A.; Feagan, B.; Panaccione, R.; Glasgow, K. W.; Fernandes, A.; Ghosh, S. Inflammatory Bowel Disease: A Canadian Burden of Illness Review. *Can. J. Gastroenterol.* **2012**, *26*, 811–817.

(15) Burisch, J.; Jess, T.; Martinato, M.; Lakatos, P. L. The Burden of Inflammatory Bowel Disease in Europe. *J. Crohn's Colitis*. **2013**, 322–337.

(16) Marchetti, M.; Liberato, N. L. Biological Therapies in Crohn's Disease: Are They Cost-Effective? A Critical Appraisal of Model-Based Analyses. *Expert Rev. Pharmacoecon. Outcomes Res*. **2014**, 815–824.

(17) Park, S. J.; Kim, W. H.; Cheon, J. H. Clinical Characteristics and Treatment of Inflammatory Bowel Disease: A Comparison of Eastern and Western Perspectives. *World J. Gastroenterol*. **2014**, 11525–11537.

(18) Ng, S. C.; Tang, W.; Ching, J. Y.; Wong, M.; Chow, C. M.; Hui, A. J.; Wong, T. C.; Leung, V. K.; Tsang, S. W.; Yu, H. H.; Li, M. F.; Ng, K. K.; Kamm, M. A.; Studd, C.; Bell, S.; Leong, R.; de Silva, H. J.; Kasturiratne, A.; Mufeena, M. N. F.; Ling, K. L.; Ooi, C. J.; Tan, P. S.; Ong, D.; Goh, K. L.; Hilmi, I.; Pisespongsa, P.; Manatsathit, S.; Rerknimitr, R.; Aniwan, S.; Wang, Y. F.; Ouyang, Q.; Zeng, Z.; Zhu, Z.; Chen, M. H.; Hu, P. J.; Wu, K.; Wang, X.; Simadibrata, M.; Abdullah, M.; Wu, J. C.; Sung, J. J. Y.; Chan, F. K. L. Incidence and Phenotype of Inflammatory Bowel Disease Based on Results from the Asia-Pacific Crohn's and Colitis Epidemiology Study. *Gastroenterology* **2013**, *145*, 158–165.

(19) Sood, A.; Midha, V.; Sood, N.; Bhatia, A. S.; Avasthi, G. Incidence and Prevalence of Ulcerative Colitis in Punjab, North India. *Gut* **2003**, *52*, 1587–1590.

(20) Tozun, N.; Atug, O.; Imeryuz, N.; Hamzaoglu, H. O.; Tiftikci, A.; Parlak, E.; Dagli, U.;

Ulker, A.; Hulagu, S.; Akpinar, H.; Tuncer, C.; Suleymanlar, I.; Ovunc, O.; Hilmioglu, F.; Aslan, S.; Turkdogan, K.; Bahcecioglu, H. I.; Yurdaydin, C. Clinical Characteristics of Inflammatory Bowel Disease in Turkey: A Multicenter Epidemiologic Survey. *J. Clin. Gastroenterol.* **2009**, *43*, 51–57.

(21) Victoria, C. R.; Sassak, L. Y.; Nunes, H. R. de C. Incidence and Prevalence Rates of Inflammatory Bowel Diseases, in Midwestern of São Paulo State, Brazil. *Arq. Gastroenterol.* **2009**, *46*, 20–25.

(22) Fakhoury, M.; Negrulj, R.; Mooranian, A.; Al-Salami, H. Inflammatory Bowel Disease: Clinical Aspects and Treatments. *J. Inflamm. Res*. **2014**, 113–120.

(23) Mowat, C.; Cole, A.; Windsor, A.; Ahmad, T.; Arnott, I.; Driscoll, R.; Mitton, S.; Orchard, T.; Rutter, M.; Younge, L.; Less, C.; Ho, G. T.; Satsangi, J.; Bloom, S. Guidelines for the Management of Inflammatory Bowel Disease in Adults. *Gut* **2011**, *60*, 571–607.

(24) Di Sario, A.; Bendia, E.; Schiadà, L.; Sassaroli, P.; Benedetti, A. Biologic Drugs in Crohn's Disease and Ulcerative Colitis: Safety Profile. *Curr. Drug Saf.* **2016**, *11*, 55–61.

(25) Collnot, E. -M.; Ali, H.; Lehr, C. -M. Nano- and Microparticulate Drug Carriers for Targeting of the Inflamed Intestinal Mucosa. *J. Control. Release* **2012**, *161*, 235–246.

(26) Lamprecht, A.; Rodero Torres, H.; Schafer, U.; Lehr, C. M. Biodegradable Microparticles as a Two-Drug Controlled Release Formulation: A Potential Treatment of Inflammatory Bowel Disease. *J. Control. Release* **2000**, *69*, 445–454.

(27) Lamprecht, A.; Ubrich, N.; Yamamoto, H.; Schafer, U.; Takeuchi, H.; Maincent, P.; Kawashima, Y.; Lehr, C. M. Biodegradable Nanoparticles for Targeted Drug Delivery in Treatment of Inflammatory Bowel Disease. *J. Pharmacol. Exp. Ther.* **2001**, *299*, 775–781.

(28) Teruel, A. H.; Coll, C.; Costero, A.; Ferri, D.; Parra, M.; Gaviña, P.; González-Álvarez, M.; Merino, V.; Marcos, M.; Martínez-Máñez, R.; Sancenón, F. Functional Magnetic Mesoporous Silica Microparticles Capped with an Azo-Derivative: A Promising Colon Drug Delivery Device. *Molecules* **2018**, *23*, 375.

(29) Teruel, A. H.; Pérez-Esteve, É.; González-Álvarez, I.; González-Álvarez, M.; Costero, A.

M.; Ferri, D.; Parra, M.; Gaviña, P.; Merino, V.; Martínez-Mañez, R.; Sancenón, F. Smart Gated Magnetic Silica Mesoporous Particles for Targeted Colon Drug Delivery: New Approaches for Inflammatory Bowel Diseases Treatment. *J. Control. Release* **2018**, *281*, 58–69.

(30) Sancenón, F.; Pascual, Ll,; Oroval, M.; Aznar, E.; Martínez-Máñez, R. Gated Silica Mesoporous Materials in Sensing Applications. *ChemOpen* **2015**, *4*, 418-437.

(31) Aznar, E.; Oroval, M.; Pascual, Ll.; Murguía, J. R.; Martínez-Máñez, R.; Sancenón, F. Gated Materials for On-Command Release of Guest Molecules. *Chem. Rev.* **2016**, *116*, 561-718.

(32) Llopis-Lorente, A.; Díez, P.; Sánchez, A.; Marcos, M. D.; Sancenón, F.; Martínez-Ruiz, P.; Villalonga, R.; Martínez-Máñez, R. Interactive Models of Communication at the Nanoscale Using Nanoparticles that Talk to One Another. *Nat. Commun.* **2017**, *8*, 15511.

(33) de la Torre, C.; Domínguez-Berrocal, L.; Murguía, J. R.; Marcos, M. D.; Martínez-Máñez, R.; Bravo, J.; Sancenón, F. ε-Polylysine-Capped Mesoporous Silica Nanoparticles as Carrier of the C9*h* Peptide to Induce Apoptosis in Cancer Cells. *Chem. Eur. J.* **2018**, *24*, 1890-1897.

(34) Oroval, M.; Díez, P.; Aznar, E.; Coll, C.; Marcos, M. D.; Sancenón, F.; Villalonga, R.; Martínez-Máñez, R. Self-Regulated Glucose-Sensitive Neoglycoenzyme-Capped Mesoporous Silica Nanoparticles for Insulin Delivery. *Chem. Eur. J.* **2017**, *23*, 1353-1360.

(35) de la Torre, C.; Casanova, I.; Acosta, G.; Coll, C.; Moreno, M. J.; Albericio, F.; Aznar, E.; Mangues, R.; Royo, M.; Sancenón, F.; Martínez-Máñez, R. Gated Mesoporous Silica Nanoparticles Using a Double-Role Circular Peptide for the Controlled and Targeted-Preferential Release of Doxorubicin in CXCR4-Expressin Lymphoma Cells. *Adv. Func. Mater.* **2015**, *25*, 687-695.

(36) Giménez, C.; Climent, E.; Aznar, E.; Martínez-Máñez, R.; Sancenón, F.; Marcos, M. D.; Amorós, P.; Rurack, K. Towards Chemical Communication between Gated Nanoparticles. *Angew. Chem. Int. Ed.* **2014**, *53*, 12629-12633.

(37) García-Fernández, A.; García-Laínez, G.; Ferrándiz, M. L.; Aznar, E.; Sancenón, F.; Alcaraz, M. J.; Murguía, J. R.; Marcos, M. D.; Martínez-Máñez, R.; Costero, A. M.; Orzáez, M. Targeting Inflammasome by the Inhibition of Caspase-1 Activity Using Capped Mesoporous Silica Nanoparticles. *J. Control. Release* **2017**, *248*, 60-70.

(38) Llopis-Lorente, A.; Lozano-Torres, B.; Bernardos, A.; Martínez-Máñez, R.; Sancenón, F. Mesoporous Silica Materials for Controlled Delivery Based-on Enzymes, *J. Mater. Chem. B.* **2017**, *5*, 3069-3083.

(39) Cabrera, S.; El Haskouri, J.; Guillem, C.; Latorre, J.; Beltrán-Porter, A.; Beltrán-Porter, D.; Marcos, M. D.; Amorós, P. Generalised Syntheses of Ordered Mesoporous Oxides: The Atrane Route. *Solid State Sci.* **2000**, *2*, 405–420.

(40) Lunn, G. *HPLC Methods for Recently Approved Pharmaceuticals*. John Wiley & Sons, Hoboken, New Jersey, USA, **2005**.

(41) Navarro, C.; González-Álvarez, I.; González-Álvarez, M.; Manku, M.; Merino, V.; Casabó, V. G.; Bermejo, M. Influence of Polyunsaturated Fatty Acids on Cortisol Transport through MDCK and MDCK-MDR1 Cells as Blood–Brain Barrier in Vitro Model. *Eur. J. Pharm. Sci.* **2011**, *42*, 290–299.

(42) Torres-Molina, F.; Peris, J. E.; García-Carbonell, M. C.; Aristorena, J. C.; Granero, L.; Chesa-Jiménez, J. Use of rats cronically cannulated in the jugular vein and the duodenum in pharmacokinetic studies. Effect of ether anestesia on absorption of amoxicillin. *Arzneimittelforschung* **1996**, *46*, 716-719.

(43) Mura, C.; Nacher, A.; Merino, V.; Merino-Sanjuan, M.; Carda, C.; Ruiz, A.; Manconi, M.; Loy, G.; Fadda, A. M.; Diez-Sales, O. *N*-Succinyl-Chitosan Systems for 5-Aminosalicylic Acid Colon Delivery: In Vivo Study with TNBS-Induced Colitis Model in Rats. *Int. J. Pharm.* **2011**, *416*, 145–154.

(44) Sandborn, W. J.; Hanauer, S. B. Systematic Review: The Pharmacokinetic Profiles of Oral Mesalazine Formulations and Mesalazine pro-Drugs Used in the Management of Ulcerative Colitis. *Aliment. Pharmacol. Ther.* **2003**, *17*, 29–42.

(45) Hartmann, G.; Bidlingmaier, C.; Siegmund, B.; Albrich, S.; Schulze, J.; Tschoep, K.;

Eigler, A.; Lehr, H. A.; Endres, S. Specific Type IV Phosphodiesterase Inhibitor Rolipram Mitigates Experimental Colitis in Mice. *J. Pharmacol. Exp. Ther.* **2000**, *292*, 22–30.

(46) Mladenovska, K.; Raicki, R. S.; Janevik, E. I.; Ristoski, T.; Pavlova, M. J.; Kavrakovski, Z.; Dodov, M. G.; Goracinova, K. Colon-Specific Delivery of 5-Aminosalicylic Acid from Chitosan-Ca-Alginate Microparticles. *Int. J. Pharm.* **2007**, *342*, 124–136.

(47) Oomen, A. G.; Rompelberg, C. J. M.; Bruil, M. A.; Dobbe, C. J. G.; Pereboom, D. P. K. H.; Sips, A. J. A. M. Development of an in Vitro Digestion Model for Estimating the Bioaccessibility of Soil Contaminants. *Arch. Environ. Contam. Toxicol.* **2003**, *44*, 281–287.

(48) Versantvoort, C. H. M.; Oomen, A. G.; Van de Kamp, E.; Rompelberg, C. J. M.; Sips, A. J. A. M. Applicability of an in Vitro Digestion Model in Assessing the Bioaccessibility of Mycotoxins from Food. *Food Chem. Toxicol.* **2005**, *43*, 31–40.

(49) Tozaki, H.; Fujita, T.; Komoike, J.; Kim, S. I.; Terashima, H.; Muranishi, S.; Okabe, S.; Yamamoto, A. Colon-Specific Delivery of Budesonide with Azopolymer-Coated Pellets: Therapeutic Effects of Budesonide with a Novel Dosage Form against 2,4,6-Trinitrobenzenesulphonic Acid-Induced Colitis in Rats. *J. Pharm. Pharmacol.* **1999**, *51*, 257–261.

(50) Tozaki, H.; Odoriba, T.; Okada, N.; Fujita, T.; Terabe, A.; Suzuki, T.; Okabe, S.; Muranishi, S.; Yamamoto, A. Chitosan Capsules for Colon-Specific Drug Delivery: Enhanced Localization of 5-Aminosalicylic Acid in the Large Intestine Accelerates Healing of TNBS-Induced Colitis in Rats. *J. Control. Release* **2002**, *82*, 51–61.

(51) Naeem, M.; Cao, J.; Choi, M.; Kim, W. S.; Moon, H. R.; Lee, B. L.; Kim, M.-S.; Jung, Y.; Yoo, J.-W. Enhanced Therapeutic Efficacy of Budesonide in Experimental Colitis with Enzyme/PH Dual-Sensitive Polymeric Nanoparticles. *Int. J. Nanomedicine* **2015**, *10*, 4565–4580.